UV Resonance Raman Characterization of Model Compounds of Tyr^{244} of Bovine Cytochrome *c* Oxidase in Its Neutral, Deprotonated Anionic, and Deprotonated Neutral Radical Forms: Effects of Covalent Binding between Tyrosine and Histidine†

M. Aki,‡ T. Ogura,§,|| Y. Naruta,⊥ T. H. Le,⊥ T. Sato,⊥ and T. Kitagawa*,‡,▽

School of Mathematical and Physical Science, Graduate University for Advanced Studies, Myodaiji, Okazaki, Aichi, 444-8585, Japan, Graduate School of Arts and Sciences, The University of Tokyo, Komaba, Meguro-ku, Tokyo 153-8902, Japan, Institute for Fundamental Research of Organic Chemistry, Kyushu University, 6-10-1 Hakozaki, Higashi-ku, Fukuoka, 812-8581, Japan, Center for Integrative Bioscience, Okazaki National Research Institutes, Myodaiji, Okazaki, Aichi, 444-8585, Japan, and CREST, Japan Science and Technology Corporation, Kawaguchi City, Japan

Received: July 2, 2001

A model compound of Tyr^{244}-His^{240} of bovine cytochrome *c* oxidase was synthesized and examined with UV resonance Raman (UVRR) as well as UV absorption spectroscopy and pH titration. Owing to the covalent linkage between imidazole and phenol, the pK_a of phenolic OH and imidazolic $N_\delta H$ groups were lowered by 1.1 and 2.3, respectively. UVRR measurements of *ortho*-imidazole-bound *para*-cresol (Im♦CrOH), its deprotonated anion (Im♦CrO$^-$), and deprotonated neutral radical (Im♦CrO$^\bullet$), and their imidazole perdeuterated, cresol perdeuterated, and ^{18}O derivatives allowed assignments of Raman bands to the imidazole and phenol modes. Unexpectedly, some of imidazole vibrations were resonance enhanced upon $\pi\pi^*$ transition of phenol, although they were not observed for the corresponding equimolar mixture of imidazole and *p*-cresol, indicating delocalization of π electrons between the imidazole and phenol rings via the covalent linkage. Such features were appreciably changed by incorporation of a bulky group at imidazole C^2 position, causing staggered conformation. The C−O stretching RR band was observed at 1530 cm^{-1} only for a radical state. The imidazole substituent at the C^2 position seems to increase appreciably a double bond character of the CO bond in the radical state than its absence. The Y8a band is not shifted upon deprotonation, although it was downshifted by 12 cm^{-1} for the unmodified *p*-cresol. The UVRR difference spectra of the anion and radical with regard to the neutral states are discussed in relation with the corresponding difference spectra of the enzyme.

Introduction

Cytochrome *c* oxidase (CcO) is a terminal enzyme of respiratory chain and catalyzes reduction of dioxygen to water in energy transducing membrane. X-ray crystallographic analysis has been completed with mammalian and bacterial enzymes at the same time.[1,2] Unexpectedly, the refinement of the structural analysis revealed that Tyr^{244} (The residue number is based on the bovine enzyme) in both proteins are covalently linked to His^{240} between *ortho* carbon of the hydroxyl group of phenol and ϵ-nitrogen of imidazole ring.[3,4] While His^{240} is one of the ligands of Cu_B, Tyr^{244} is located near the catalytic site of dioxygen reduction and simultaneously at the end point of a proton channel from the matrix side (K channel).[5] Judging from its location, Tyr^{244} is considered to play an acid−base catalysis similar to distal histidine of peroxidases[6] and, in addition, is proposed to be a new possible redox center, in which Tyr^{244} holds an extra oxidation equivalent in the P intermediate of its enzymatic reaction.[7] Therefore, it became quite desirable to understand the essential role Tyr^{244} plays in the catalysis by CcO and characterization of Tyr^{244} in order to understand the enzymatic reaction of CcO.

In a number of redox enzymes, such as ribonucleotide reductase,[8] prostaglandin H synthase,[9] and photosystem II (PSII),[10] Tyr radical is known to play a crucial role during the catalytic reaction. In the active site of galactose oxidase[11] and glyoxal oxidase[12] tyrosine is covalently bound with cystein. On the other hand, model systems for them have been extensively studied.[13] However, covalent linkage of Tyr with His has never been seen in other enzymes so far. Very recently, a model compound for such a system was synthesized,[14,15] but there has been no spectroscopic characterization for it, particulary for the effect of covalent binding of His on the phenol group of Tyr. If π orbital mixing occurs between the two rings via the covalent linkage, the pK_a of the O−H group of Tyr and the N−H group of His as well as the UVRR spectra of Tyr would be altered from those of unmodified Tyr and His. Accordingly, in the present study, we have synthesized *ortho*-imidazole-bound *para*-cresol [2-(1-imidazolyl)-4-methylphenol, Im♦CrOH] and its isotope derivatives, including ^{18}O derivative [Im♦Cr^{18}OH], imidazole-perdeuterated [Im(D$_3$)♦CrOH], and cresol-perdeuterated [Im♦CrOH(D$_6$)] ones, and investigated the UV resonance Raman (UVRR) spectra of their neutral, deprotonated anion [Im♦CrO$^-$], and deprotonated neutral radical [Im♦CrO$^\bullet$] forms. To see the effects of torsional distortion between the two molecular planes of imidazole and phenol rings on the properties, a derivative with a bulky group at the C^2 position of imid-

† Part of the special issue "Mitsuo Tasumi Festschrift".

* To whom correspondence should be addressed. Fax: +81−564−55−4639. Phone: +81−564−55−7340. E-mail: teizo@ims.ac.jp.
‡ School of Mathematical and Physical Science.
§ Graduate School of Arts and Sciences.
|| CREST.
⊥ Institute for Fundamental Research of Organic Chemistry.
▽ Center for Integrative Bioscience.

10.1021/jp012492n CCC: $22.00
Published on Web 01/24/2002

azole [2-(2-methyl-1-imidazolyl)-4-methylphenol, CH_3Im♦CrOH] was also synthesized.

Experimental Procedures

Acid−Base Titration. Im♦CrOH was dissolved in carbonic acid free water, which was boiled again just before use, to the concentration of 500 μM. A small portion of 2.2 mM NaOH or HCl was put dropwise into the sample solution through a buret for titration. The pH was recorded at each step with a Beckman 720 pH meter, and the pK_a was determined from the titration curve.

UVRR Spectroscopy. UVRR spectra were excited by a XeCl excimer laser-pumped dye laser system (EMG103MSC/LPX120 and FL2002/SCANMATE, Lambda Physik). The 308-nm line from the XeCl excimer laser was used to excite coumarin 480, and the 480-nm output from the dye laser was frequency-doubled with a β-BaB_2O_4 crystal to generate 240-nm pulses. The 240-nm light was focused into a diameter of ∼50 μm and led to the sample from the lower front side by a lens (f = 200 mm). Raman scattering from the illuminated spot was collected by Cassegrainian optics with F = 1.1 and focused onto the entrance slit (mechanical slit width: 200 μm) of the double monochromator (SPEX 1404, f = 850 mm, F = 7.8) by an achromatic lens (f = 150 mm). Raman scattered light was dispersed with the asymmetrical double monochromator in which the first and second dispersion steps were based on the first-order use of a 2400 grooves/mm (holographic) grating and the second-order use of a 1200 grooves/mm (machine-ruled, 500-nm blaze) grating, respectively.[16] The dispersed light was detected by an intensified photodiode array (PC−IMD/C5222−0110G, Hamamatsu). The photocathode and linear image sensor were cooled to −15 and −25 °C, respectively. To avoid sample destruction by illumination of UV laser, the spinning cell (1800 rpm) with stirring function[17] was used; the inside magnet bar of the spinning cell, which was a small handmade hemidisk magnet (diameter = 1.5 mm, thickness = 2.0 mm), was made to stand still during spinning of the cell by a strong outside magnet placed at the backside of the laser incidence. The Raman spectra were measured at 30 °C.

For the measurements of neutral and deprotonated anion (phenolate) states, the laser system was operated to produce pulses with a peak power of ∼25 μJ/pulse (∼1.3 J/cm^2 pulse) at 100 Hz. For the measurements of phenoxyl radical state, the peak power of laser was increased to ∼1.3 mJ/pulse (∼66 J/cm^2 pulse) by operating it at 10 Hz. The observed spectra contained the contributions from the phenoxyl radicals and phenolates. The contribution from the phenolate, obtained with a low laser power for the same solution, was digitally subtracted from the observed high-power spectra to obtain the spectrum of phenoxyl radicals.[18] At the laser illuminated point, a yield of phenoxyl radical was estimated to be ca. 70−80% in this experiment. Under this illumination condition, the bands of a dimerization photoproduct, such as *p*,*p*-biphenol, were not recognized in the spectra of the radical form.

Raman shifts were calibrated with dioxane and a mixture of cyclohexane/trichloroethylene (cyclohexane:trichloroethylene = 4:1 (v/v)), whose Raman bands obtained with a visible laser were calibrated with indene. The wavenumber coverage by the detector was approximately 630 cm^{-1}, and thus the wavenumber resolution was ∼0.8 cm^{-1}/pixel. The sensitivity differences at individual pixels were corrected by the use of a D_2 standard lamp (Hamamatsu, model C1518 and model H4141SV). Raman intensity correction for self-absorption[19] and intensity normalization were carried out with the 980 cm^{-1} band of SO_4^{2-} ion contained in the sample solution.

UV Absorption Spectroscopy. Im♦CrOH was dissolved in distilled water to the final concentration of 25 μM, the pH of which was adjusted by adding NaOH or HCl solution. CH_3Im♦CrOH was treated in the same way, but its concentration was appreciably higher than that of Im♦CrOH. Optical absorption spectra of these solutions were recorded with a Hitachi U-3210 spectrophotometer.

^{1}H NMR Spectra. ^{1}H NMR spectra were recorded on a JEOL LMX-GX400 (400 MHz). Chemical shifts are reported in ppm (δ) relative to tetramethylsilane (TMS) in $CDCl_3$, and coupling constants (J) were indicated in Hz.

Mass Spectra. Electrospray ionization mass spectra (ESI-MS) were obtained on a Perkin-Elmer Sciex API-300 mass spectrometer. Scanning was in 0.1-dalton steps and a 10 ms dwell time per step. The orifice voltage was controlled from −50 to +60 V, dependent on the intensity of TIC. GC-mass spectra were obtained on a JEOL JMS-AM SUN 200 spectrometer. High-resolution mass (HR-MS) spectra were recorded on a JEOL JMS−HX-110 spectrometer. FAB-MS spectra were measured with 3-nitrobenzyl alcohol as a matrix.

FT-IR Spectra. FT-IR spectra were recorded on a JEOL JIR-Winspec 50 spectrometer.

Elemental Analyses. Elemental analyses were performed at Analysis Center in Kyushu University.

Materials. All reagents and solvents were of the reagent grade and were used without further purification unless otherwise noted. D_4-Imidazole (95 atom % D) and DCl (37 wt % in D_2O, 99.5 atom % D) were obtained from Aldrich Chemical Co., Wisconsin. D_6-*p*-Cresol (97.9 atom % D) was purchased from CDN Isotopes, Quebec, Canada. Labeled dioxygen $^{18}O_2$ (isotope enrichment, 95%) was obtained from Cambridge Isotope Laboratories, MA. Dry reagents were obtained by the procedures described below. Tetrahydrofuran (THF) was dried over KOH and distilled from Na/benzophenone. Dichloromethane (CH_2Cl_2) was stirred with concentrated sulfuric acid for several days and dried over K_2CO_3, and then it was distilled from CaH_2. Acetone was dried over Drierite and used after distillation. Trichloroethylene and sodium sulfate were purchased from Nacalai Tesque, Japan. The spectral grade dioxane and cyclohexane were purchased from Dojin Kagaku Laboratory, Japan. Synthesis of [2-(1-imidazolyl)-4-methylphenol, Im♦CrOH] is based on the reported method.[20]

Synthesis of **2-Bromo-*p*-cresol Benzyl Ether (2a).** A mixture of 2-bromo-*p*-cresol (**1a**, 15.0 g, 53.5 mmol), and benzyl chloride (10.63 g, 56 mmol), K_2CO_3 (22.2 g, 139.0 mmol) in dry acetone (100 mL) was refluxed overnight under N_2 atmosphere. After filtration of the solid material, the solvent was evaporated in vacuo. The residue was passed through an alumina layer (eluent, benzene) to afford the benzyl ether (**2a**, 37.03 g, 87.7%). ^{1}H NMR 2.26 (s, 3H, Me), 5.12 (s, 2H, CH_2Ph), 6.81(d, 1H, J = 8.3, cresol H^6), 7.00 (dd, 1H, J = 8.3, 1.5, cresol H^5), 7.31 (t, 1H, J = 7.3, Ph H$^{4'}$), 7.37 (t, 2H, J = 7.3, Ph H$^{3',5'}$), 7.38 (s, 1H, cresol H^3), 7.46 (d, 2H, J = 7.3, Ph H$^{2',6'}$). HR-MS found 276.0150. Calcd for $C_{14}H_{13}O_{79}Br$ 279.0150.

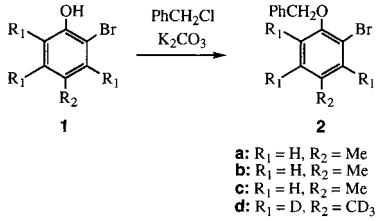

1 **2**

a: R_1 = H, R_2 = Me
b: R_1 = H, R_2 = Me
c: R_1 = H, R_2 = Me
d: R_1 = D, R_2 = CD_3

Synthesis of 2-(2-Methyl-1-imidazolyl)-4-methylphenyl Benzyl Ether (4b). The mixture of 2-bromo-*p*-cresole benzyl ether (**2a**, 5.54 g, 20.0 mol), 2-methylimidazole (**3b**, 1.642 g, 20.0 mmol), K_2CO_3 (3.04 g, 22.0 mmol), and Cu powder (279 mg) was heated at 200 °C for 3 h under nitrogen atmosphere. The reaction mixture was treated with aq NaOH and extracted with $CHCl_3$. After evaporation of the extract in vacuo, the residue was chromatographed on silica gel (eluent, $CHCl_3$:MeOH = 30:1) to give **4b** (2.51 g, 45%). ^{1}H NMR 2.24 (s, 3H, CH_3−Im), 2.33 (s. 3H, CH_3−Ph), 5.02 (s, 2H, CH_2), 6.91 (d, 1H, J = 1.5, Im-H^4), 6.97 (d, 1H, J = 8.3, cresol-H^6), 7.02 (d, 1H, J = 1.5, Im-H^5), 4.04 (d, 1H, J = 2, cresol-H^3), 7.15 (dd, 1H, J = 2 and 8, cresol-H^5), 7.20 (d, 2H, J = 7, Ph-H^{2,6}), 7.27−7.33 (m, 3H, Ar-H). HR-MS found 279.1485. Calcd for $C_{18}H_{19}ON_2$, 279.1474.

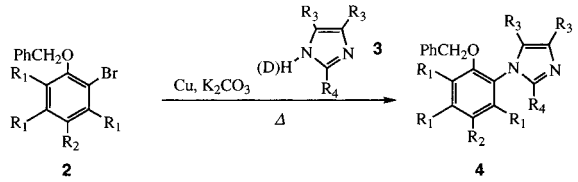

a: R_1 = H, R_2 = Me, R_3 = R_4 = H
b: R_1 = H, R_2 = Me, R_3 = H, R_4 = Me
c: R_1 = H, R_2 = Me, R_3 = R_4 = D
d: R_1 = D, R_2 = CD_3, R_3 = R_4 = H

Synthesis of 2-(2-Methyl-1-imidazolyl)-4-methylphenol (5b, CH_3−Im♦CrOH**).** A mixture of **4b** (2.224 g, 8.0 mmol), 5% Pd−C (150 mg), snf concentrated HCl (300 mL) in EtOH (150 mL) was hydrogenated at atmospheric pressure. After the calculated amount of hydrogen was absorbed for 5.5 h, the catalyst was filtered and washed with EtOH. The filtrate was concentrated in vacuo, added aq $NaHCO_3$ and the solution was extracted with chloroform. After the organic layer was dried, it was evaporated in vacuo and the residue was purified by column chromatography (silica gel, *i*-PrOH:$CHCl_3$ = (1−2):10), The fractions which contained the desired product were subjected to another chromatographic purification using alumina and $CHCl_3$ to give **5b** (488 mg, 32%); mp >165 °C (sublimed). NMR 2.23 (s, 3H, CH_3-Im), 2.29 (s, 3H, CH_3-Ph), ≈6.5 (br, 1H, OH), 6.90 (s, 2H, imidazole ring H), 6.92 (d, 1H, J = 1.5, H^3), 7.05 (d, 1H, J = 8.3, H^6), 7.09 (dd, 1H, J = 1.5, 8.3, H^5). HR-MS found 189.1093. Calcd for $C_{11}H_{13}ON_2$, 189.1028.

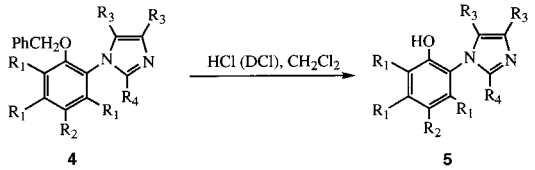

a: R_1 = H, R_2 = Me, R_3 = R_4 = H
b: R_1 = H, R_2 = Me, R_3 = H, R_4 = Me
c: R_1 = H, R_2 = Me, R_3 = R_4 = D
d: R_1 = D, R_2 = CD_3, R_3 = R_4 = H

Synthesis of 2-{2-Methyl-1-[2′, 4′, 5′−D_3]imidazolyl}-4-methylphenyl Benzyl Ether (4c). The mixture of **2a** (5.65 g, 20.0 mol), D_4-imidazole (**3c**, 1.438 g, 19.94 mmol), K_2CO_3 (3.58 g, 25.95 mmol), and Cu powder (279 mg) was heated at 200 °C for 75 min under nitrogen atmosphere. The reaction mixture was treated with aq NaOH and extracted with $CHCl_3$. After evaporation of the extract in vacuo, the residue was chromatographed on alumina (eluent, benzene:$CHCl_3$ = 1:1) to give **4c** as an oil in 91.5% yield (4.876 g, 18.26 mmol). NMR 2.24 (s, 3H, Me), 2.33 (s, 3H, Me), 5.02(s, 2H, CH_2), 6.91 (1H, J = 1.5, Im-H^4), 6.98 (d, 1H, J = 8.3), 7.03 (d, 1H, J = 1.5, Im C −H), 7.04 (d, 1H, J = 2.0), 7.09 (dd, 1H, J = 1.5, 14), 7.17 (d, 2H, J = 2), 7.20 (dd, 2H, J = 1.5, 7.1, 2,6-H), 7.27−7.33 (m, 5H, arom-H).

Synthesis of 2-{1-[2′, 4′, 5′[D_3]imidazolyl}-4-methylphenol (5c, Im(D_3)♦CrOH**).** A mixture of **4c** and 36% DCl in D_2O in CH_2Cl_2 (10 mL) was stirred at room-temperature overnight. The aqueous layer was separated and neutralized with aq $NaHCO_3$ and the resultant solution was dried up in vacuo. The residue was treated with a small amount of CH_2Cl_2 in several times. The product was purified by flash chromatography on silica gel (eluent, *i*-PrOH:$CHCl_3$ = (1−2):10) to give **5c**. The proton signals assignable to imidazole ring protons were not observed and the deuterium content at these positions was estimated to be >95%; mp 124−125 °C. ^{1}H NMR 2.30 (s, 3H, CH_3), 7.01 (br, 1H, H^3), 7.04 and 7.05 (each br, 2H, H,^{5} H^6). HR-MS found 178.1090. Calcd for $C_{10}H_8D_3ON_2$, 178.1120.

Synthesis of *p*-[^{18}O]Cresol. Magnesium shot (1.5 g) was ground in a 100-mL three-necked flask under heating and nitrogen atmosphere for 12 h and dry THF (10 mL) was added after cooling to room temperature. A portion of *p*-bromotoluene (11 g, 64.3 mmol) in dry THF (5 mL) was introduced and warmed gently until the reaction started. Then the rest of the mixture was added and stirred for 1 h. The Grignard reagent was transferred to a 25-mL flask equipped with a three-way stopcock. To the flask was added $^{18}O_2$ (140 mL, 5.73 mmol), and the mixture was stirred for 2 days. The flask was cooled with an ice bath, and water, HCl, and $NaHSO_3$ solution were added to it. The mixture was extracted with CH_2Cl_2, washed with aqueous $NaHCO_3$, and dried over anhydrous Na_2SO_4, and the drying agent was filtered. The filtrate was concentrated, and the residue was chromatographed on silica gel (eluent, CH_2Cl_2), which afforded the desired cresol. This process was repeated twice to give *p*-[^{18}O]cresol (518 mg, 40% yield based on the amount of the applied $^{18}O_2$). The ^{18}O content in the cresol was determined to be 90% by GC-MS. ^{1}H NMR 2.28 (s, 3 H, −CH_3), 4.59 (s, 1 H, −OH), 6.73 (d, 2 H, J = 8.6, H^{2,6}), 7.04 (d, 2H, J = 8.6, H^{3,5}). GC-MS m/z = 107 (10.6), 108 (10.3), 109 (100), 110 (80.7), 111 (8.1). IR (KBr) 3307, 3021, 2921, 2865, 1513, 1220, 815 cm^{-1}. Found C 76.47, H 7.34. Calcd for $C_7H_8{}^{18}O$, C 76.33, H 7.32.

Synthesis of 2-Bromo-*p*-[^{18}O]cresol (1a-^{18}O). To a stirred CCl_4 (10 mL) solution of *p*-[^{18}O]cresol (449 mg, 4.08 mmol) was added a CCl_4 solution of bromine (679 mg, 4.25 mmol) dropwise at −15 °C. After the addition, the mixture was allowed to react for another 10 min. A 10% $NaHSO_3$ solution was added to the mixture and the reaction mixture was extracted with CH_2Cl_2. The combined organic layers were washed with aqueous $NaHCO_3$, dried over anhydrous $MgSO_4$, and then filtered. The filtrate was concentrated to give **1a**-^{18}O (546 mg, 71%) as a clear oil. ^{1}H NMR 2.27 (s, 3H, −CH_3), 5.33 (s, 1H, −OH), 6.91 (d, J = 8.3, 1H, Ar-H), 7.02 (d, J = 8.3, 1H, Ar-H), 7.27 (s, 1H, Ar-H). IR (KBr) 3500, 3027, 2923, 2861, 1494, 1178, 815 cm^{-1}. Found C 43.85, H 3.74. Calcd for $C_7H_7{}^{18}OBr\cdot 0.2H_2O$, C 43.64, H 3.87.

Synthesis of 2-Bromo-*p*-[^{18}O]cresol Benzyl Ether (2a-^{18}O). The mixture of 2-bromo-*p*-[^{18}O]cresol (**1a**-^{18}O, 546 mg, 2.89 mmol), benzyl chloride (550 mg, 4.34 mmol), and K_2CO_3 (1 g, 7.24 mmol) in DMF (6 mL) was stirred at 60 °C overnight. After cooling of the vessel to a room temperature and filtration of the solid, the mixture was extracted with ethyl acetate. The organic layer was washed with 1 M HCl and brine, and then was dried over anhydrous Na_2SO_4, filtered, and evaporated. Chromatography of the residue on silica gel (eluent, hexane) afforded **2a**-^{18}O (760 mg, 95%). ^{1}H NMR 2.27 (s, 3 H, −CH_3),

5.13 (s, 2 H, $-CH_2O-$), 6.82 (d, $J = 8.3$, 1 H, Ar-H), 7.01 (d, $J = 6.8$, 1 H, Ar-H), 7.31−7.48 (m, 6 H, Ar-H); IR (KBr) 3062, 3031, 2915, 1492, 1245 cm^{-1}. Found C 60.27, H 4.69. Calcd for $C_{14}H_{13}{}^{18}OBr$, C 60.23, H 4.69.

Synthesis of 2-(1-Imidazolyl)-4-methylphenyl Benzyl [^{18}O]-Ether (4a-^{18}O). The bromide derivative (**2**-^{18}O, 645 mg, 2.31 mmol), imidazole (180 mg, 2.64 mmol), copper (243 mg, 3.82 mmol), and K_2CO_3 were placed in a 10-mL flask equipped with a three-way stopcock. The mixture was heated at 200 °C for 1 h under N_2 with gentle stirring. After cooling of the vessel, the mixture was dissolved in aqueous HCl, and then basified with aqueous NaOH. The mixture was extracted with CH_2Cl_2, dried, and evaporated. Column chromatographic purification of the residue on alumina (eluent, $CHCl_3$) gave **4a**-^{18}O (442 mg 72%). ^{1}H NMR 2.34 (s, 3 H, $-CH_3$), 5.07 (s, 2 H, $-CH_2O-$), 6.99−7.34 (m, 10 H, Ar-H, Im-H^{4,5}), 7.82 (s, 1 H, Im-H^2). IR (KBr) 3031, 2919, 1519, 1226, 736 cm^{-1}. Found C 75.35, H 6.01, N 10.37. Calcd for $C_{17}H_{16}N_2{}^{18}O\cdot 0.3H_2O$, C 75.14, H 6.16, N 10.31.

Synthesis of 2-(1-Imidazolyl)-4-methyl[^{18}O]phenol (5a-^{18}O, Im♦Cr^{18}OH). Under N_2 were added **4a**-^{18}O (155 mg, 0.58 mmol), concentrated HCl (4 mL), and CH_2Cl_2 (1.5 mL) to a 25-mL flask. After the mixture was stirred at room temperature for 10 h, it was neutralized with K_2CO_3. The solution was extracted with CH_2Cl_2, and the organic layer was dried over Na_2SO_4. After filtration of the solid, the filtrate was concentrated under reduced pressure. Column chromatographic purification of the residue (silica gel, CH_2Cl_2:*i*-PrOH = 10:1) gave **5a**-^{18}O (53 mg, 52%). The^{18}O-isotope purity in the product was determined to be 89% from the peak strength of the fragments in FAB mass spectrum: ^{1}H NMR 2.31 (s, 3 H, $-CH_3$), 7.01−7.15 (m, 5 H, Ar-H and Im-H^{4,5}), 7.72 (s, 1 H, Im-H^2). HR-MS found 177.0914. Calcd for $C_{10}H_{11}N_2{}^{18}O$ 177.0914; IR (KBr) 3122, 1519, 1280, 825 cm^{-1}. Found C 68.11, H 5.79, N 15.68. Calcd for $C_{10}H_{10}N_2{}^{18}O$, C 68.16, H 5.72, N 15.90.

Synthesis of 2-Bromo-*p*-[3, 5, 6, α, α, α-D$_6$]cresol (1d). Bromine (1.55 mL, 30 mmol) in CCl_4 (10 mL) was slowly added at −10 to −15 °C to a CCl_4 solution (20 mL) of *p*-[D_8]cresol (3.45 g, 29.7 mmol). After removal of the solvent at reduced pressure, the residual oil was practically pure **1d** (5.761 g, 100%). HR-MS found 193.0135. Calcd for $C_7H_2D_6BrO$ $[M+H]^+$ 193.0136.

Synthesis of 2-Bromo-*p*-[3, 5, 6, α, α, α-D$_6$]cresol Benzyl Ether (2d). An acetone solution (60 mL) of **1d** (5.55 g, 28.6 mmol) and benzyl chloride (3.45 mL, 29.9 mmol) was refluxed overnight with K_2CO_3 (8.1 g). Workup and purification was done as compound **3a** to give **3d** (7.90 g, 97.7%). ^{1}H NMR 5.13 (s, 2H, OCH_2), 7.32 (*t*, 1H, $J = 7.3$, H^4 of Ph), 7.39 (*t*, 2H, $J = 7.3$, H^{3,5} of Ph), 7.48 (d, 2H, $J = 7.3$, H^{2,6} of Ph). HR-MS found 283.0603. Calcd for $C_{14}H_8D_6BrO$ $[M+H]^+$ 283.0605.

Synthesis of 2-(1-Imidazolyl)-4-[D$_3$]methyl[D$_3$]phenyl Benzyl Ether (4d). The bromide **2d** (5.66 g, 20.0 mmol), imidazole (1.498 g, 22 mmol), copper (345 mg, 3.82 mmol) and K_2CO_3 (4.146 g, 30 mmol) were placed in a 10-mL flask equipped with a three-way stopcock. The mixture was heated at 200 °C for 1 h under N_2 with gentle stirring. After the vessel was cooled, the mixture was dissolved in aqueous HCl, and then basified with aqueous NaOH. The mixture was extracted with CH_2Cl_2, dried, and evaporated. Column chromatographic purification of the residue on alumina (eluent, $CHCl_3$) gave **4d** (4.518 g, 83%); mp 56−59 °C. ^{1}H NMR 5.12 (s, 2H, CH_2), 7.1−7.4 (6H, m, Ph ring-H and Im-H^4 or H^5), 7.48 (br, 1H, Im-H^4 or H^5), 8.69 (br, 1H, Im-H^2). HR-MS found 271.1715. Calcd for $C_{17}H_{11}D_6N_2O$ $[M+H]^+$ 271.1717.

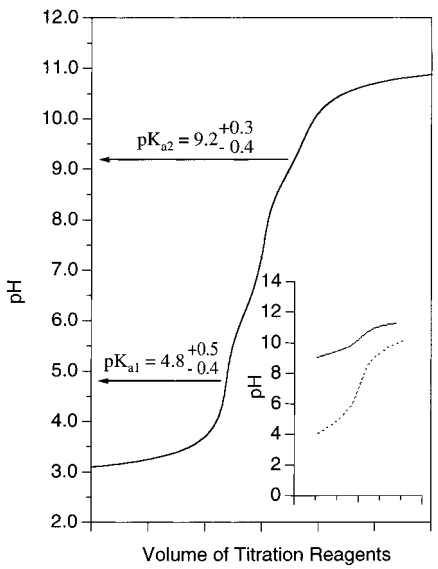

Figure 1. Acid−base titration curve of 2-(1-imidazolyl)-4-methylphenol. The pH reading is plotted against the volume of 2.2 mM NaOH or HCl added to 500 μM solution of Im♦CrOH. The inset illustrates similar titration curves obtained for *p*-cresol (solid line) and imidazole (broken line) with the same method.

Synthesis of 2-(1-Imidazolyl)-4-[D$_3$]methyl[D$_3$]phenol (5d, Im♦Cr(D$_6$)OH). Under N_2, to a 25-mL flask were added **4d** (403 mg, 0.58 mmol), concentrated HCl (4 mL), and CH_2Cl_2 (1.5 mL). After the mixture was stirred at room temperature for 10 h, the pH of the solution was adjusted to be 7 with aq NaOH. The solution was extracted with CH_2Cl_2, and the organic layer was dried over Na_2SO_4. After filtration of the solid, the filtrate was concentrated under reduced pressure. Column chromatographic purification of the residue (silica gel, CH_2Cl_2: *i*-PrOH = 10:1) gave **5d** (110 mg, 41%). The proton signals assignable to cresol ring and methyl protons were not observed and the deuterium content at these positions was estimated to be >95%; mp 164−166 °C. ^{1}H NMR 8.25 (bs, 1H, Im-H^2), 7.27 (s, 2H, Im-H^4 and H^5), ≈ 5.5 (br, 1H, OH). Anal. ($C_{10}H_{16}N_2O$) C, H, N. HR-MS found 181.1247. Calcd for $C_{10}H_4D_6N_2O$ $[M+H]^+$ 181.1248.

Results

The acid−base titration curve of Im♦CrOH is depicted in Figure 1, where the pH reading of the solution is plotted against the added volume of reagent. This allowed us to determine the pK_a values of phenolic OH group to be 9.2 (9.5 > pK_a > 8.8) and of imidazolic N$_\delta$H group to be 4.8 (5.3 > pK_a > 4.4). Similar titration curves for *p*-cresol and imidazole are delineated in the inset and they gave pK_a values of 10.3 ± 0.3 and 7.1 ± 0.3 for *p*-cresol and imidazole, respectively. Thus, the covalent linkage of imidazole group lowers pK_a of the phenolic OH group by 1.1. Although this is slightly smaller than the value determined by McCauley et al.[14] who found that, upon the lowering of pK_a of phenol by 1.6, the direction of changes are the same, whereas both are opposite to the ordinary expectation: when an electron donating group is attached at *ortho*-position of OH, its pK_a should be raised by an inductive effect. The pK_a lowering is attributed to the stabilization of phenolate anion by π donation from the covalently bound imidazole. On the other hand, the pK_a of imidazole moiety of Im♦CrOH is lowered by 2.3. This modulation means the increased acidity

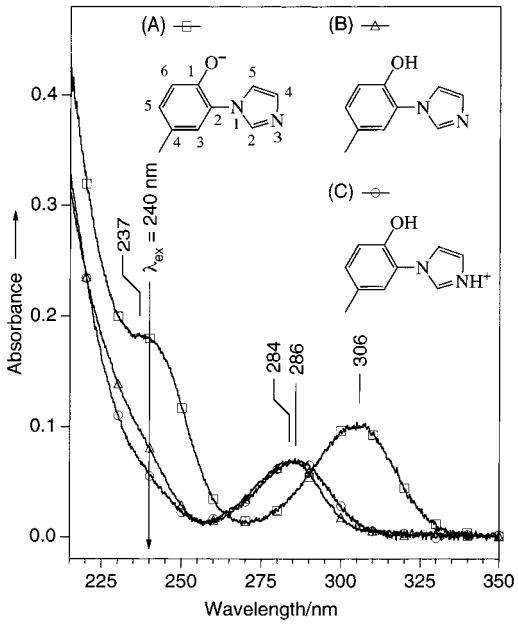

Figure 2. UV absorption spectra of 2-(1-imidazolyl)-4-methylphenol at pH 11 (Im♦CrO^-, A), at pH 7.0 (Im♦CrOH, B), at pH 3.0 (ImH^+♦CrOH, C). Experimental conditions; light path length, 1 cm; sample concentration, 25 μM. Raman excitation wavelength is denoted by an arrow. Molecular structures of Im♦CrO^-, Im♦CrOH, and ImH^+♦CrOH are illustrated schematically in the blank space.

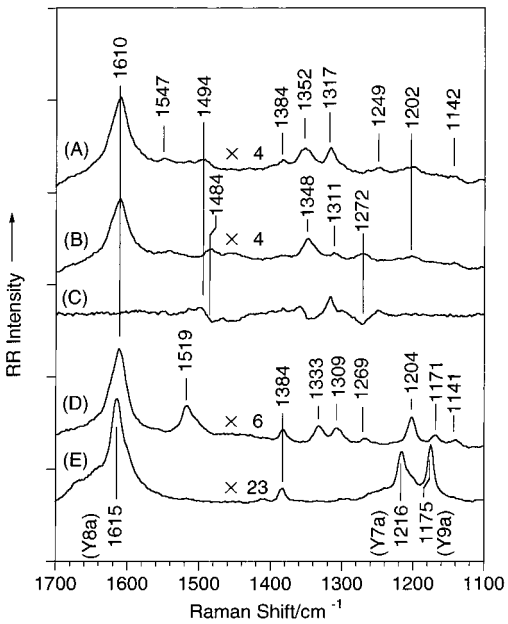

Figure 3. UVRR spectra of neutral forms; Raw spectra of Im♦CrOH (A), $Im(D_3)$♦CrOH (B), CH_3Im♦CrOH (D), and *p*-cresol (E) at pH 6.4 (100 mM sodium phosphate buffer) and the isotopomer difference spectrum regarding imidazole perdeuteration (C = A − B). Experimental conditions: laser pulse energy, ~25 μJ/pulse; repetition rate, 100 Hz; sample concentrations, 1.7 mM for Im♦CrOH, 0.84 mM for CH_3Im♦CrOH, and 2.5 mM for *p*-cresol. Raman intensity is normalized with the 980 cm^{-1} line of SO_4^{2-} ion [240 mM(SO_4^{2-})/mM(unmodified and modified *p*-cresol)] present in the solution among the spectra within this figure and also with those in Figures 4 and 5. The spectra are expanded in the ordinate direction by a factor designated for each spectrum (*x* number). The true intensity is 1/number.

at both sides of imidazole and phenol, suggesting the increased π delocalization between phenol and imidazole rings.

Electronic absorption spectra of Im♦CrO^- (A), Im♦CrOH (B), and ImH^+♦CrOH (C) are shown in Figure 2 where the observed spectra of the same compound at pH 11, pH 7.0, and pH 3.0 are depicted. For convenience sake, molecular structures of the anion, neutral, and cation forms are schematically illustrated in the empty space of Figure 2. The absorption maxima of the anion are red-shifted relative to those of the neutral and cation states, indicating that these absorptions arise from the phenol moiety. The feature at 237 nm is peculiar to the anion state and assigned to the La ($^1B_{1u}$) transition of *para*-substituted phenol, while the Lb ($^1B_{2u}$) transition was observed at 284, 286 and 306 nm for the neutral, cation, and anion states, respectively. The absorption spectra of CH_3Im♦CrOH (not shown) were similar to those of Im♦CrOH, although the corresponding absorption maxima of the La bands were slightly shifted to shorter wavelengths (283, 283, and 303 nm).

The 240-nm excited UVRR spectra of neutral forms observed at pH 6.4 are shown in Figure 3, where raw spectra of Im♦CrOH (A), $Im(D_3)$♦CrOH (B), CH_3Im♦CrOH (D), and *p*-cresol (E) and the difference between the imidazole-deuterated and the parent molecules (C = A − B) are included. The UVRR spectrum of Im♦$Cr^{18}OH$ (not shown) was same as that of Im♦CrOH, meaning that the vibrations associated with the C−OH group (C−OH stretch (Y7a′), ~1260 cm^{-1}) are too weak to be identified. In fact, only the band at 1610 cm^{-1} is clearly observed for Im♦CrOH among three major bands of *p*-cresol which are identified at 1615 (Y8a), 1216 (Y7a), and 1175 cm^{-1} (Y9a) in spectrum (E). Here, the vibrational assignments of *p*-cresol are based on Takeuchi and Harada:[21] Y8a, phenol ring C═C stretching, Y9a, CH in-plane bending, and Y7, phenol ring C−C stretching mixed with CH in-plane bending.

However, additional bands are present in the spectrum of Im♦CrOH (A) at 1494, 1352, 1317, and 1249 cm^{-1}. The corresponding bands of the imidazole-perdeuterated compound are seen at shifted positions with slightly different intensities in spectrum (B). This is more clearly seen in the isotope difference spectrum (C). Therefore, these bands are assigned to imidazole vibrations. When an equimolar mixture of imidazole and *p*-cresol were subjected to UVRR measurements under the same conditions, only the Raman bands of *p*-cresol were observed. This means that some of imidazole vibrations gain resonance enhancement of Raman intensity upon $\pi\pi^*$ transition of phenol ring, suggesting appreciable mixing of π electrons between the two rings via the covalent linkage.

It is not clear how much they are mixed. It would depend on the coplanarity of the phenol and imidazole rings. If it were coplanar in Im♦CrOH, incorporation of a bulky group to the C^2 position of imidazole would cause some distortion toward a staggered conformation. Comparison of spectrum (D) with spectrum (A) reveals the effect of such distortion. New bands appear at 1519 and 1171 cm^{-1}, while the bands at 1333, 1309, and 1269 cm^{-1} are intensified and slightly shifted. The appearance of Y7a at 1204 cm^{-1} and of Y9a at 1171 cm^{-1} may suggest closer approach to the isolated phenol moiety, but the intensification of imidazole bands is contradictory to it. The apparent intensification might be caused by narrowing of bands in spectrum (D) than in spectrum (A), implying that the structure is more widely distributed in the absence of the bulky group at C^2 of imidazole.

The 240-nm excited UVRR spectra of deprotonated anion forms are shown in Figure 4, where raw spectra of Im♦CrO^- (A), $Im(D_3)$♦CrO^- (B), Im♦$CrO(D_6)^-$ (D), CH_3Im♦CrO^- (F), and *p*-cresolate (G), and the isotopomer differences regarding imidazole-deuteration (*C* = A − B) and phenol-deuteration (*E* = A − D) are included. The RR bands of *p*-cresolate (G) are seen at 1603 (Y8a), 1559 (Y8b), 1384, 1208 (Y7a), and 1172

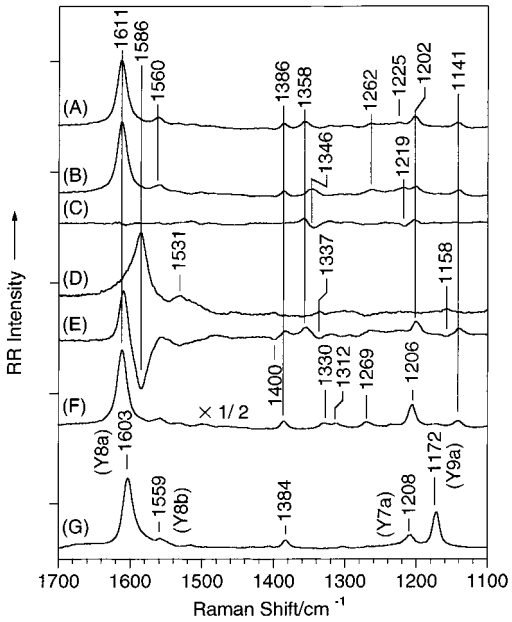

Figure 4. UVRR spectra of anion forms; Raw spectra of Im♦CrO^- (A), $Im(D_3)$♦CrO^- (B), Im♦$CrO(D_6)^-$ (D), CH_3Im♦CrO^- (F), and *p*-cresolate (G) at pH 13 (100 mM NaOH aq) and the isotopomer difference spectra regarding imidazole perdeuteration ($C = A - B$), and cresol perdeuteration ($E = A - D$). Experimental conditions: laser pulse energy, ~25 μJ/pulse; repetition rate, 100 Hz. Sample concentration and intensity normalization are the same as those in the caption of Figure 3.

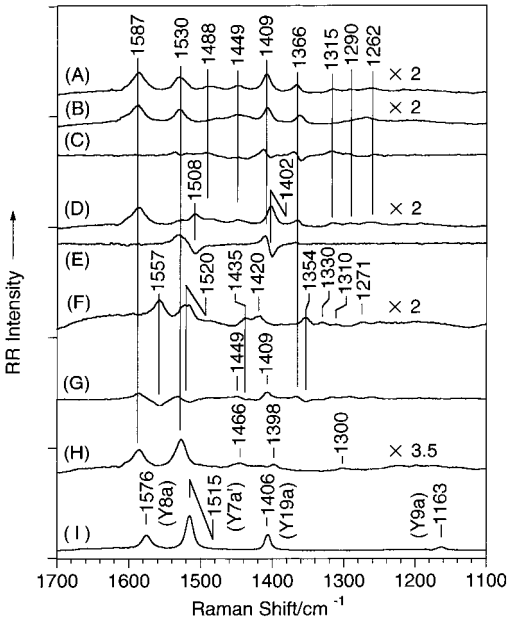

Figure 5. UVRR spectra of radical forms; Raw spectra of Im♦$CrO^•$ (A), $Im(D_3)$♦$CrO^•$ (B), Im♦$Cr^{18}O^•$ (D), Im♦$CrO(D_6)^•$ (F), CH_3Im♦$CrO^•$ (H), and *p*-cresoxyl radical (I) at pH 13 (100 mM NaOH aq) and the isotopomer difference spectra regarding imidazole perdeuteration ($C = A - B$), ^{18}O substitution ($E = A - D$), and cresol perdeuteration ($G = A - F$). Experimental conditions: laser pulse energy, ~1.3 mJ/pulse; repetition rate, 10 Hz; Sample concentration and intensity normalization are the same as those in the caption of Figure 3.

cm^{-1} (Y9a) for which the assignments are based on Takeuchi and Harada.[21]

The bands at 1358, 1262, 1225, and 1202 cm^{-1} in spectrum (A) are not seen in spectrum (G). Among them, the bands at 1358 and 1202 cm^{-1} are shifted to 1346 and 1219 cm^{-1} upon perdeuteration of imidazole, while the band at 1202 cm^{-1} is present but weakened in spectrum (B) as more clearly indicated by the difference spectrum (C). Presumably all of them arise from mainly imidazole ring modes. It is noted, however, that the band at 1202 cm^{-1} in spectrum (A) is an overlapped band, while this band in spectrum (B) is purely due to a phenol ring. On the other hand, the bands of spectrum (A) at 1611, 1560, 1386 and 1141 cm^{-1} exhibit neither a frequency shift nor an intensity change upon imidazole deuteration. In contrast, perdeuteration of cresol caused frequency shifts of the bands at 1611, 1560, 1386, 1358, and 1141 cm^{-1} to 1586, 1531, 1400, 1337, and 1158 cm^{-1}, respectively, and disappearance of Y7a band at 1202 cm^{-1} as indicated by the difference spectrum (E). These bands are no doubt assigned to the phenol modes. The high-frequency shift of the 1141 cm^{-1} band would be due to deletion of the contribution of the C−H in-plane bending mode to Y9a in perdeuterated *p*-cresol. It was unexpected that the imidazole mode at 1358 cm^{-1} exhibited a frequency shift upon *p*-cresol deuteration, but it means occurrence of vibrational mixing between some of imidazole and phenyl modes. As an effect of staggered conformation the bands at 1330, 1312, 1269, and 1206 cm^{-1} in spectrum (F) are intensified in comparison with those in spectrum (A) but the band at 1358 cm^{-1}, which is evident in the spectrum (A), disappears. The Y8a intensity of CH_3Im♦CrO^- in spectrum (F) is nearly twice strong as Y8a of Im♦CrO^- (A), indicating that more staggered conformation reduces more the effect of covalent binding of imidazole. Thus, these bands reflect the difference in the mixing of phenolic π orbitals with imidazolic π orbitals.

Surprisingly, the UVRR spectrum observed for Im♦$Cr^{18}O^-$ (not shown) was the same as that of Im♦CrO^-, indicating the absence of ^{18}O sensitive mode in UVRR spectrum. Furthermore, the Y8a frequency of Im♦CrO^- (1611 cm^{-1}) is almost the same as that of Im♦CrOH (1610 cm^{-1}, Figure 3A), despite the fact that the Y8a frequency of cresolate (1603 cm^{-1}, Figure 4G) is distinctly lower than that of cresol (1615 cm^{-1}, Figure 3E).

The UVRR spectra of deprotonated neutral radical forms are illustrated in Figure 5, where raw spectra of Im♦$CrO^•$ (A), $Im(D_3)$♦$CrO^•$ (B), Im♦$Cr^{18}O^•$ (D), Im♦$Cr(D_6)O^•$ (F), CH_3Im♦$CrO^•$ (H), and *p*-cresoxyl radical (I), and differences regarding imidazole deuteration ($C = A - B$), ^{18}O-substitution ($E = A - D$), and cresol deuteration ($G = A - F$) are delineated. The RR bands of *p*-cresoxyl radical at 1576 (Y8a), 1515 (Y7a′), 1406 (Y19a) and 1163 cm^{-1} (Y9a) in spectrum (I) were assigned on the basis of the 399-nm-excited Raman spectra reported by Tripathi and Schuler.[22] The corresponding bands of Im♦$CrO^•$ are seen at 1587 (Y8a), 1530 (Y7a′), and 1409 (Y19a) cm^{-1}, but Y9a is too weak to identify. In addition to them, bands are observed at 1488, 1449, 1366, 1315, 1290, and 1262 cm^{-1} in spectrum (A). These bands exhibit complicated difference patterns upon imidazole deuteration (C), indicating that they arise mainly from the imidazole moiety. It means that imidazole vibrations are weakly resonance enhanced upon $\pi\pi^*$ transition of the phenol ring as pointed out for the neutral and anion states. It is stressed that the phenol modes at 1530 and 1409 cm^{-1} also gave clear differential patterns in trace (C). This demonstrates that the C−H in-plane deformation modes of imidazole are appreciably mixed with phenyl ring modes.

The ^{18}O substitution of phenol ring of Im♦$CrO^•$-caused frequency shifts of two bands at 1530 and 1409 cm^{-1} to 1508 and 1402 cm^{-1}, respectively, but other bands were hardly affected as shown by difference spectrum (E). Previously, Spiro and co-workers[23] examined 245-nm excited RR spectra of ^{17}O-substituted phenoxyl radical and observed a downshift of 13 cm^{-1} for Y7a′. In spectrum (D) the 1508 cm^{-1} band is

downshifted by 22 cm^{-1} from that in spectrum (A). It is reasonable that the size of this shift is nearly double of the ^{17}O isotopic frequency shift, demonstrating that the 1530 cm^{-1} mode involves primarily the C−O stretching character. However, the 1409 cm^{-1} band of Im♦CrO• also exhibits a downshift of 7 cm^{-1} upon ^{18}O substitution which is smaller than the double of the ^{17}O isotopic shift (7 cm^{-1}). This means that the Y19a mode also contains the C−O stretching character, but its content is nearly one-third of that of Y7a′.

Upon perdeuteration of cresol, the phenyl modes at 1587, 1530, and 1409 cm^{-1} of Im♦CrO• are shifted to 1557, 1520, and 1420 cm^{-1}. The shifts can be reasonably understood on the basis of vibrational mixing of C−H in-plane deformation modes in the C−H compound. However, the frequency shifts of imidazole modes of Im♦CrO• at 1449 and 1366 cm^{-1} to 1435 and 1354 cm^{-1}, respectively, are unexpected. This again indicates the vibrational mixing of imidazole and phenol modes. Incorporation of a bulky group at the C^2 position of imidazole changed the relative intensity of Y8a to Y7a′ and as a result, the spectral pattern became closer to that of *p*-cresoxyl radical than the case without the steric hindrance, although the Y19a is significantly weakened in CH_3Im♦CrO•.

Discussion

Radical Form. The Y7a′ has been observed around 1505−1517 cm^{-1} regions for the radical state of phenoxyl and its 4-substituted phenoxyl derivatives (XC_6H_4O•, X = H, CH_3, F, Cl, Br), and they are categorized into phenoxyl-like.[24] The Y8a has been observed around 1552−1577 cm^{-1} for the pheoxyl-like radicals. On the other hand, for *p*-aminophenoxyl radical ($H_2NC_6H_4O$•) and *p*-hydroxyphenoxyl (*p*-benzosemiquinone) anion radical ($^-OC_6H_4O$•), the Y7a′ have been observed in the lower frequency region (1434 and 1435 cm^{-1})[25,26] than those of the phenoxyl-like,[24] whereas the Y8a have been observed in the higher frequency region (1636 and 1620 cm^{-1}, respectively).[25,26] These are categorized as the semiquinone anion-like.[24] The bond order of the CO bond is influenced by migration of the p(π) electrons from the substituent group to the CO group via the ring. In the phenoxyl ground state, there is apparently an effective migration of electrons from the ring p(π) system to the CO group, which would impart a double bond character to the CO bond and correspondingly transfer the unpaired electron density mainly to the highest occupied orbital of the phenyl ring. This feature was demonstrated with ESR which indicated the spin population on the phenol ring to be ∼0.8.[27] In the ground state of semiquinone anions, the migration of the p(π) electrons from the substituents (−NH_2 or −O^-) to the CO group occurs via the phenyl ring,[28] and as a result the unpaired electron density is almost equally shared by the CO group and the substituent, resulting in the decrease of the CO bond order.[24] For *p*-methoxyphenoxyl and *p*-benzosemiquinone radicals (XC_6H_4O•, X = OCH_3 or OH), Y8a is observed at 1607 and 1613 cm^{-1}, and Y7a′ is observed at 1518 and 1511 cm^{-1}, respectively,[24,25] and thus the phenyl ring is semiquinone anion-like but the CO bond is still phenoxyl-like. For the radical state of 2-X-4-methyl-disubstituted phenoxyl derivatives (XC_7H_6O•, X = CH_3 and SCH_3), Y7a′ is observed at 1516 and 1518 cm^{-1} and Y8a is observed at 1585 and 1582 cm^{-1}.[11d] These frequencies are closer to being phenoxyl-like than to being semiquinone anion-like.

For Im♦CrO• (Figure 5A), the Y8a frequency (1587 cm^{-1}) is categorized as being phenoxyl-like, whereas the Y7a′ frequency (1530 cm^{-1}) is remarkably higher than that for 4-substituted phenoxyl radicals (1505−1518 cm^{-1}). In the imidazole-substituted phenol, the migration of electrons from the phenol ring π system to the CO group might be more efficient and might give more double bond character to the CO bond than to that of other substituents (−H, −CH_3, −F, −Cl, −Br, and −SCH_3). This might be one of important effects of covalent binding of His to Tyr in the enzyme. It is noted that the Y8a and Y7a′ frequencies of Im♦CrO• are the same as those of CH_3♦Im CrO• (Figure 5H), indicating that the C−O bond order is not affected by a change of the π orbital mixing between the phenol and imidazole rings in the ground state.

A distinct effect of the radical formation on the UVRR spectra of *p*-cresol is seen in the relative intensity of Y8a to Y7a′ bands; Y7a′ is very weak for the neutral (Figure 3E) and anion (Figure 4G) forms, whereas Y7a′ is stronger than Y8a for the radical form (Figure 5I). This feature is retained in the Im♦CrOH system (compare Figures 3A, 4A, with 5A), and is considered to be the property of *para*-substituted phenol.[18,23,29] This is partly due to more mixing of C−O stretch with Y8a vibration (intensity borrowing), but is essentially caused by the excited-state geometry.[24]

The relative intensity of Y8a and Y7a′ bands is altered by incorporation of a CH_3 group to the C^2 position of imidazole (compare Figure 5A with Figure 5H). Similar relative intensity changes of the two bands have been observed for 4-substituted and 4,2-disubstituted phenoxyl radicals,[24,11d] too. It is thought that when electron migration from the π(p) orbital of the substituent to the phenol ring occurs in the excited state, the Y8a band is more strongly resonance enhanced than the Y7a′ band.[24] In spectra (A) and (H) in Figure 5, although their relative intensities are reversed, their frequencies remained unaltered. Since the Raman intensity reflects an excited electronic state but frequencies reflect the ground electronic state, it is likely that the donation of π electrons from the imidazole ring occurs more in Im♦CrO than in CH_3Im♦CrO and the effect is more pronounced in the La excited state than in the ground state. This is presumably caused by the difference in coplanarity of the phenole and imidazole rings between Im♦CrO and CH_3Im♦CrO.

The Y19a vibration appears around 1400 cm^{-1} for phenoxyl and 4-substituted phenoxyl radicals.[24] The difference band at 1409 cm^{-1} in spectrum Figure 5C means that the in-plane C−H deformation character of imidazole is mixed with the Y19a mode of phenol. The Y19a frequency becomes slightly lower and its intensity becomes weaker in the staggered conformation as seen in spectrum Figure 5H. This band shows the phenol-^{18}O isotopic frequency shift of 7 cm^{-1}, which is smaller than the value (14 cm^{-1}) expected from the ^{17}O isotopic frequency shift.[23] Thus, the extent of mixing of C−O stretching character with Y19a is influenced by the covalent bond of imidazole to phenol and the dihedral angle between them.

Figure 6 shows the UVRR spectra of neutral (Im♦CrOH) and radical forms (Im♦CrO•) and their difference. When Tyr^{244} becomes a neutral radical state in the P intermediate, this kind of difference spectrum with regard to the neutral oxidized form is expected. A large negative peak at 1610 cm^{-1} and several positive peaks with medium intensity at 1587, 1530, and 1409 cm^{-1} are expected upon excitation at 240 nm. Although these peaks have not been observed for the enzyme despite of the expectation that Tyr^{244} becomes a neutral radical in the P intermediate,[7] identification of the corresponding peaks in the UVRR spectra of CcO intermediates is desirable in immediate future.

Anion Form. Generally, the Y8a band of anion form is much stronger than that of the neutral form upon excitation around

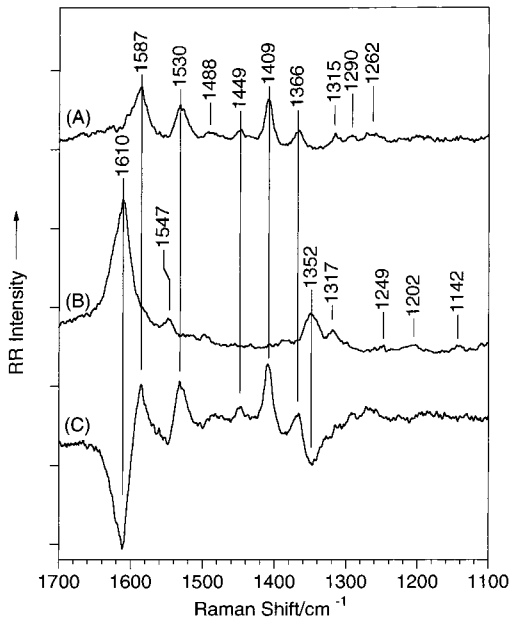

Figure 6. Comparison of the 240-nm excited RR spectra of Im♦CrO• (A) and Im♦CrOH (B) and their 1:1 difference spectrum (C).

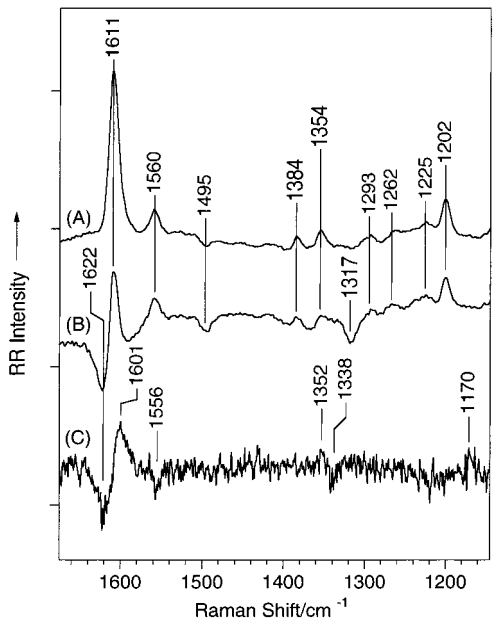

Figure 7. The difference spectra between Im♦CrO$^-$ and Im♦CrOH. Trace A was obtained from the 1:1 difference calculation and trace B was obtained by weighting 1:2.8. Trace C shows the pH difference spectrum (pH 9.1−6.1) of bovine cytochrome *c* oxidase in the oxidized state which was reproduced from Figure 5(C) in ref 17.

240 nm, and its frequency is lower in the anion form.[16] In fact, for the unmodified *p*-cresol, theY8a intensity of the anion form (Figure 4G) is stronger by ∼23 times than that of the neutral form (Figure 3E), and the Y8a frequency is lower in the anionic form by 12 cm^{-1}. However, the situation is sensitively altered by the modification of *p*-cresol. The Y8a intensity of Im♦CrO$^-$ (Figure 4A) is stronger only by 4 times than that of the neutral form (Figure 3A). Figure 7 illustrates their difference spectra, Im♦CrO$^-$ minus Im♦CrOH. Trace (A) was obtained with 1:1 difference calculation: that is, Figure 7A = Figure 4A − Figure 3A. This is expected in the difference spectrum of the enzyme when Tyr^{244} is simply deprotonated without any conformational change. Actually, however, the pH difference spectrum of bovine CcO,[17] is not compatible to it as reproduced by trace (C) in Figure 7. In a model system, only positive peaks appear at the positions of Im♦CrO$^-$. This is owing to significant intensification of Raman bands of Im♦CrO$^-$. When the difference calculation was carried out with weighting factors of 1:2.8 for Im♦CrO$^-$:Im♦CrOH, the resultant difference spectrum, which is delineated by trace (B) in Figure 7, becomes closer to the enzyme pH-difference spectrum (C). We point out that the feature of phenol ring modes of model compounds should occur in the enzyme to reproduce the pH-difference spectrum of Tyr^{244}.

If this is the case, the UVRR spectrum of Tyr^{244} in the enzyme should be more intensity reduced in the anion form than in the neutral form. A possible origin of the intensity reduction would be a change in the dihedral angle between the phenol and imidazole planes; more planar in the alkaline form than in the neutral form. This is a likely phenomenon in the enzyme system, if deprotonation of phenol is involved under fixed geometry of the imidazole moiety due to Cu_B. It is noted that the negative peak at 1622 cm^{-1} in the model is not due to the presence of a peak at 1622 cm^{-1} in the neutral form. It is on account of the difference in bandwidth: the 1610 cm^{-1} band of the neutral form (Figure 3A) is much broader due to structural inhomogeneity than the 1611 cm^{-1} band of the deprotonated anion form (Figure 4A). It is stressed that the corresponding difference peak was observed in the pH difference spectrum of the enzyme (pH 9.1 minus pH 6.1) only for the fully oxidized form, but not for the fully reduced and the fully reduced CO-bound forms,[17] indicating that the oxidation−reduction reaction of heme a_3 causes no protonation/deprotonation of Tyr^{244}. In a mutant hemoglobin (Hb M Iwate), we proved that the conversion of TyrO$^-$/TyrOH for the tyrosine residue located near heme *b* is caused by the oxidation state of the metal ion, that is, heme b^{3+}/heme b^{2+}, by UVRR spectroscopy.[30]

According to the X-ray crystallographic analysis of Im♦CrOH, the torsion angle between the phenolic and imidazolic rings is reported to be 42.3°.[31] This angle is almost the same as the dihedral angle of the Tyr^{244} and His^{240} rings, which was determined by X-ray crystallographic analysis of the fully oxidized CcO.[3] The corresponding angles of the deprotonated forms have not been determined for both the enzyme and the model compound in alkaline conditions, and there is still a possibility that the angle is different between crystal and aqueous solution.

In conclusion, the covalent linkage between Tyr^{244} and His^{240} allows significant delocalization of π electrons between phenol and imidazole rings. This may provide a base for EPR silence of the P intermediate even if Tyr^{244} radical is formed when Cu(II) is coordinated His^{240}. In the present model compound, a metal ion is not coordinated to N_δ of imidazole but Cu_B is coordinated to His^{240} in the enzyme. This would affect the UVRR intensity in the neutral, anion, and radical forms of phenol moiety of Im♦CrOH, and therefore should be taken into consideration when the present results are compared with those from the enzyme.

Acknowledgment. This work was supported by Grants-in-Aid for Scientific Research in Priority Area to T.K. (12045264), T.O. (11169210), and for COE research to Y.N. (08CE2005) from the Ministry of Education, Science, Sports, and Culture, Japan.

References and Notes

(1) Tsukihara, T.; Aoyama, H.; Yamashita, E.; Tomizaki, T.; Yamaguchi, H.; Shinzawa-Itoh, K.; Nakashima, R.; Yaono, R.; Yoshikawa, S. *Science* **1996**, *272*, 1136−1144.

(2) Iwata, S.; Ostermeier, C.; Ludwig, B.; Michel, H. *Nature* **1995**, *376*, 660−669.

(3) Yoshikawa, S.; Shinzawa-Itoh, K.; Nakashima, R.; Yaono, R.; Yamashita, E.; Inoue, N.; Yao, M.; Fei, M. J.; Libeu, C. P.; Mizushima, T.; Yamaguchi, H.; Tomizaki, T.; Tukihara, T. *Science* **1998**, *280*, 1723−1729.

(4) Iwata S. *Biochemistry* **1998**, *123*, 369−375.

(5) (a) Thomas, J. W.; Puustinen, A.; Alben, J. O.; Gennis, R. B.; Wikstrom, M. *Biochemistry* **1993**, *32*, 10923−10928. (b) Fetter, J. R.; Qian, J.; Shapleigh, J.; Thomas, J. W.; Garcia-Horsman, A.; Schmidt, E.; Hosler, J.; Babcock, G. T.; Gennis, R. B.; Ferguson-Miller, S. *Proc. Natl. Acad. Sci. U.S.A.* **1995**, *92*, 1604−1608. (c) Garcia-Horsman, A.; Puustinen, A.; Gennis, R. B.; Wikstrom, M. *Biochemistry* **1995,** *34*, 4428−4433. (d) Gennis, R. B. *Biochim. Biophys. Acta*, **1998**, *1365*, 241−248.

(6) Uchida, T.; Mogi, T.; Kitagawa, T. *Biochemistry* **2000,** *39*, 6669−6678.

(7) Proshlyakov, D. A.; Pressler, M. A.; DeMaso, C.; Leykam, J. F.; DeWitt, D. L.; Babcock, G. T. *Science* **2000**, *290*, 1588−1591.

(8) (a) Sjöberg, B. M.; Larson, A. *EMBO J.* **1986**, *5*, 2037−2040. (b) Bollinger, J. M., Jr.; Edmondson, D. E.; Huynh, B. H.; Filley, J.; Norton, J. R.; Stubbe, J. *Science* **1991**, *253*, 292−298.

(9) (a) Karthein, R.; Dietz, R.; Nastainczyk, W.; Ruf, H. H. *Eur. J. Biochem.* **1998**, *171*, 313−320. (b) Smith, W. L.; Eling, T. E.; Kulmacz, R. J.; Marnett, L. J.; Tsai, A. *Biochemistry* **1992**, *31*, 3−7.

(10) (a) Barry, B. A.; El-Deeb, M. K.; Sandusky, P. O.; Babcock, G. T. J. *Biol. Chem.* **1990**, *265*, 20139−20143. (b) Hoganson, C. W.; Babcock, G. T. *Biochemistry* **1992**, *31*, 11874−11880.

(11) (a) Ito, N.; Phillips, S. E. V.; Yadav, K. D. S.; Knowles, P. F. *J. Mol. Biol*. **1994**, *238*, 794. (b) Whittaker, M. M.; Ballou, D. P.; Whittaker, J. W. *Biochemistry* **1998**, *37*, 8426. (c) Wachter, R M.; Montague-Smith, M. P.; Branchaud, B. P. *J. Am. Chem. Soc.* **1997**, *119*, 7743. (d) McGlashen M. L.; Eads, D. D.; Spiro, T. G.; Whittaker, J. W. *J. Phys. Chem*. **1995**, *99*, 4918−4922.

(12) Whittaker, M. M.; Kersten, P. J.; Nakamura, N.; Sanders-Loehr, J.; Schweizer, E. S.; Whittaker, J. W. *J. Biol. Chem*. **1996**, *271*, 681.

(13) (a) Itoh, S.; Taki, M.; Kumei, H.; Takayama, S.; Nagatomo, S.; Kitagawa, T.; Sakurada, N.; Arakawa, R.; Fukuzumi, S. *Inorg. Chem*. **2000,** *39*, 3708−3711. (b) Halfen, J. A.; Jazdzewski, B. A.; Mahapatra, S.; Berreau, L. M.; Wilkinson, E. C.; Que, L. Jr.; Tolman, W. B.; *J. Am. Chem. Soc*. **1997**, *119*, 8217. (c) Wang, Y.; DuBois, J. L.; Hedman, B. Hodgson, K. O.; Stack, T. D. P. *Science* **1998,** *279*, 537. (d) Chaudhuri, P.; Hess, M.; Muller, J.; Hildenbrand, K.; Bill, E.; Weyhermuller, T.; Wieghardt, K. *J. Am. Chem. Soc*. **1999,** *121*, 9599. (e) Sokolowski, A.; Müller, J.; Weyhermüller, T.; Schnepf, R.; Hildebrandt, P., Hildenbrand, K.; Bothe, E.; Wieghardt, K. *J. Am. Chem. Soc*. **1997**, *119*, 8889−8900. (f) Schnepf, R.; Sokolowski, A.; Müller, J.; Bachler, V.; Wieghardt, K.; Hildebrandt, P. *J. Am. Chem. Soc.* **1988**, *120*, 2352−2364.

(14) McCauley, K. M.; Vrtis, J. M.; Dupout, J.; van der Donk, W. A., *J. Am Chem Soc*. **2000**, *122*, 2403−2404.

(15) (a) Collman, J. P.; Zhong, M.; Wang, Z. *Org. Lett.* **1999**, *1(6)*, 949−951. (b) Elliott, G. I.; Konopelski, J. P. *Org. Lett.* **2000**, *2(20)*, 3055−3057. (c) Collman, J. P.; Wang, Z.; Zhong, M.; Zeng, L. *J. Chem. Soc., Perkin Trans.* **2000**, *1*, 1217−1221.

(16) Kaminaka, S.; Kitagawa, T. *Appl. Spectrosc.*, **1992**, *46*, 1804.

(17) Aki, M.; Ogura, T.; Shinzawa-Itoh, K.; Yoshikawa, S.; Kitagawa, T., *J. Phys. Chem. B.* **2000**, *104*, 10765.

(18) Johnson, C. R.; Ludwig, M.; Asher, S. A. *J. Am. Chem. Soc.* **1986**, *108*, 905−912.

(19) Fodor, S. P. A.; Rava, R. P.; Hays, T. R.; Spiro, T. G. *J. Am. Chem. Soc.* **1985**, *107*, 1520.

(20) Strehlke, P. *Eur. J. Med. Chem.* **1979**, *14*, 227.

(21) Takeuchi, H.; Harada, I. *J. Raman Spectosc.* **1990**, *21*, 509.

(22) Tripathi, G. N. R.; Schuler, R. H. *J. Chem. Phys.* **1984**, *81*, 113−121.

(23) Mukherjee, A.; McGlashen, M. L.; Spiro, T. G. *J. Phys. Chem.* **1995**, *99*, 4912.

(24) (a) Tripathi, G. N. R.; Schuler, R. H. *J. Phys. Chem.* **1988**, *92*, 5129−5133. (b) Tripathi, G. N. R. *Time-Resolved Spectroscopy*; Clark, R. J. H., Hester, R. E., Eds.; John Wiley & Sons: Chichester, *Adv. Spectrosc.* **1989**, *18*, 175−192.

(25) Tripathi, G. N. R.; Schuler, R. H. *J. Phys. Chem*. **1987**, *91*, 5881.

(26) Tripathi, G. N. R.; Schuler, R. H. *J. Phys. Chem*. **1984**, *88*, 1706.

(27) Neta, P.; Fessenden, R. W. *J. Phys. Chem*. **1974**, *78*, 523.

(28) Pauling, L. *The Nature of the Chemical Bond*; Cornell University Press: Ithaca, New York, 1960; p 357.

(29) Rava, R. P.; Spiro, T. G. *J. Phys. Chem.* **1985**, *89*, 1856−1861.

(30) Nagai, M.; Aki, M.; Li, R.; Jin, Y.; Sakai, H.; Nagatomo, S. Kitagawa, T. *Biochemistry* **2000**, *39*, 13093−13105.

(31) Naruta, Y.; Tachi, Y.; Chishiro, T.; Shimazaki, Y.; Tani, F. *Acta Crystallogr*. **2001**, *Sect. E 57*, 550−552.